

ANL-HEP-CP-97-32

hep-ph/9708408

## ISOLATED PROMPT PHOTON PRODUCTION \*

CONF-970393--

EDMOND L. BERGER<sup>a</sup>, XIAOFENG GUO<sup>b</sup>, and JIANWEI QIU<sup>c</sup>

<sup>a</sup>*High Energy Physics Division, Argonne National Laboratory,*

*Argonne, IL 60439, USA*

<sup>b</sup>*Physics Department, Columbia University,*

*NY, NY 10027, USA*

<sup>c</sup>*Department of Physics and Astronomy, Iowa State University,*

*Ames, IA 50011, USA*

(August 15, 1997)

RECEIVED  
SEP 22 1997  
CERN

### Abstract

We show that the conventionally defined partonic cross section for the production of isolated prompt photons is not an infrared safe quantity. We work out the case of  $e^+e^- \rightarrow \gamma + X$  in detail, and we discuss implications for hadron reactions such as  $p\bar{p} \rightarrow \gamma + X$ .

DISTRIBUTION OF THIS DOCUMENT IS UNLIMITED

MASTER

The submitted manuscript has been authored by a contractor of the U. S. Government under contract No. W-31-109-ENG-38. Accordingly, the U. S. Government retains a nonexclusive, royalty-free license to publish or reproduce the published form of this contribution, or allow others to do so, for U. S. Government purposes.

\*Invited paper presented by E. L. Berger at the XXXIIInd Rencontres de Moriond, *QCD and High Energy Hadronic Interactions*, Les Arcs, Savoie, France, March 22 - 29, 1997.

## **DISCLAIMER**

This report was prepared as an account of work sponsored by an agency of the United States Government. Neither the United States Government nor any agency thereof, nor any of their employees, makes any warranty, express or implied, or assumes any legal liability or responsibility for the accuracy, completeness, or usefulness of any information, apparatus, product, or process disclosed, or represents that its use would not infringe privately owned rights. Reference herein to any specific commercial product, process, or service by trade name, trademark, manufacturer, or otherwise does not necessarily constitute or imply its endorsement, recommendation, or favoring by the United States Government or any agency thereof. The views and opinions of authors expressed herein do not necessarily state or reflect those of the United States Government or any agency thereof.

## **DISCLAIMER**

**Portions of this document may be illegible  
in electronic image products. Images are  
produced from the best available original  
document.**

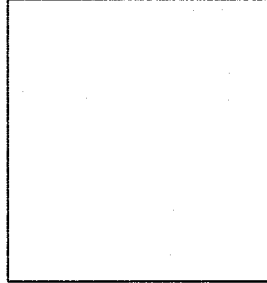
# ISOLATED PROMPT PHOTON PRODUCTION

EDMOND L. BERGER<sup>a</sup>, XIAOFENG GUO<sup>b</sup>, and JIANWEI QIU<sup>c</sup>

<sup>a</sup>*High Energy Physics Division, Argonne National Laboratory,  
Argonne, IL 60439, USA*

<sup>b</sup>*Physics Department, Columbia University,  
NY, NY 10027, USA*

<sup>c</sup>*Department of Physics and Astronomy, Iowa State University,  
Ames, IA 50011, USA*



We show that the conventionally defined partonic cross section for the production of isolated prompt photons is not an infrared safe quantity. We work out the case of  $e^+e^- \rightarrow \gamma + X$  in detail, and we discuss implications for hadron reactions such as  $p\bar{p} \rightarrow \gamma + X$ .

## 1 Terminology

### 1.1 Photon Isolation

In  $e^+e^-$  and in hadron-hadron reactions at collider energies, prompt photons are observed and their cross sections are measured only if the photons are relatively isolated in phase space. Isolation is required to reduce various hadronic backgrounds including those from the electromagnetic decay of mesons, e.g.,  $\pi^0 \rightarrow 2\gamma$ . The essence of isolation is that a cone of half-angle  $\delta$  is drawn about the direction of the photon's momentum, and the isolated cross section is defined for photons accompanied by less than a specified amount of hadronic energy in the cone, e.g.,  $E_h^{\text{cone}} \leq E_{\text{max}} = \epsilon_h E_\gamma$ ;  $E_\gamma$  denotes the energy of the photon. Instead of  $\delta$ , the Fermilab collider groups use the variable  $R = \sqrt{(\Delta\phi)^2 + (\Delta\eta)^2}$ , where  $\Delta\eta$  and  $\Delta\phi$  denote differences of rapidity and azimuthal angle variables. Theoretical predictions will therefore depend upon the additional parameters  $\epsilon_h$  and  $\delta$  (or  $R$ ). The *isolated* cross section is not an *inclusive* cross section, and, as we discuss below, the usual factorization theorems for inclusive cross sections do not apply. Isolation removes backgrounds, but it also reduces the signal. For example, it reduces the contribution from processes in which the photon emerges from the long-distance fragmentation of quarks and gluons, themselves produced in short-distance hard collisions.

## 1.2 Conventional Factorization

Much of the predictive power of perturbative QCD derives from factorization theorems<sup>1</sup>. *Conventional* factorization expresses a physical quantity as the convolution of a partonic term with a nonperturbative long-distance matrix element. It requires that the partonic term, calculated perturbatively order-by-order in the the strong coupling strength  $\alpha_s$ , have no infrared singularities, and that the long-distance matrix element be universal. Applied to the case of  $e^+e^- \rightarrow AX$ , conventional factorization states

$$\sigma_{e^+e^- \rightarrow A+X}(Q) = \hat{\sigma}_{e^+e^- \rightarrow c+X}(x, Q/\mu) \otimes D_{c \rightarrow A}(z, \mu) + O\left(\frac{1}{Q}\right). \quad (1)$$

The intermediate state  $c$  may be a quark, antiquark, gluon, or photon. The symbol  $\otimes$  denotes a convolution. Variable  $z = p_A/p_c$ . The fragmentation function  $D_{c \rightarrow A}(z, \mu)$  represents long-distance, small momentum scale physics; its dependence on the fragmentation scale  $\mu$  is governed by the Altarelli-Parisi evolution equations. In situations in which the factorization theorem applies, the partonic hard-part (“the partonic cross section”)  $\hat{\sigma}_{e^+e^- \rightarrow c+X}(x, Q/\mu)$  is infrared safe, i.e., finite when all infrared regulators are removed.

Conventional factorization holds for *inclusive* prompt photon production  $e^+e^- \rightarrow \gamma X$ , demonstrated through next-to-leading order<sup>2</sup>. However, since the isolated cross section is not an inclusive quantity, factorization need not hold and indeed does not<sup>3</sup>. Nevertheless, almost all existing calculations of the cross section for isolated photon production assume its validity<sup>4</sup>. Following the standard calculational procedures of perturbative quantum chromodynamics (QCD), we show that the partonic hard-part for the isolated photon cross section is not infrared safe. The infrared sensitivity shows up first in the next-to-leading order quark-to-photon fragmentation contribution<sup>3</sup>. We use the terminology “breakdown of conventional factorization” to describe this result.

## 2 Photons in $e^+e^-$ Annihilation, $e^+e^- \rightarrow \gamma + X$

Electron-positron reactions offer a relatively clean environment for the study of prompt photon production in hadronic final states<sup>5</sup>. Since there are no complications from initial state hadrons,  $e^+e^- \rightarrow \gamma + X$  is a good process in which to examine QCD predictions in the final state, and the data may be a good source of information on quark-to-photon and gluon-to-photon fragmentation functions<sup>6,7,8</sup>. In turn, these fragmentation functions are needed for predictions of photon yields in hadronic collisions. Hard photons in  $e^+e^-$  processes arise as QED bremsstrahlung from the initial beams, radiation that is directed along angles near  $\theta_\gamma = 0$  and  $\pi$ , and as final state radiation from *direct* and *fragmentation* processes. The topic of interest in this paper is the final state radiation. It populates all angles, with an angular distribution having both transverse,  $1 + \cos^2 \theta_\gamma$ , and longitudinal components<sup>2</sup>.

Cataloging the contributions to  $e^+e^- \rightarrow \gamma + X$ , we may first list the lowest order partonic process:  $e^+e^- \rightarrow q + \bar{q}$ , followed by quark or antiquark fragmentation into a photon,  $q \rightarrow \gamma X$ . The  $\mathcal{O}(\alpha_{em})$  direct contribution is represented by the three-body final state process  $e^+e^- \rightarrow q + \bar{q} + \gamma$ . Separation of the lowest order fragmentation and the  $\mathcal{O}(\alpha_{em})$  direct contributions is not unique; the fragmentation scale  $\mu$  dependence relates the two. At  $\mathcal{O}(\alpha_s)$  the contributions of interest come from the three-body final state processes  $e^+e^- \rightarrow q + \bar{q} + g$ , followed by gluon fragmentation,  $g \rightarrow \gamma X$ ; and from  $e^+e^- \rightarrow q + \bar{q} + g$ , followed by quark or antiquark fragmentation,  $q \rightarrow \gamma X$ . In Fig. 1(a) and 1(b), we illustrate the set of Feynman diagrams used in the computation of the contribution from  $e^+e^- \rightarrow q + \bar{q} + g$  (with the implied understanding that the final quark or antiquark fragments into a photon). The set of real gluon emission diagrams in Fig. 1(a) results in an infrared sensitive contribution, associated with the region of phase space in which the emitted gluon momentum becomes soft. Likewise, the set of virtual gluon loop diagrams in Fig. 1(b) also results in an infrared sensitive contribution. In the case of *inclusive* photon production, the infrared singularities cancel once the results from the two sets are combined. However, in the *isolated* photon case, the restriction on the phase space accessible to the final state gluon in the set of Fig. 1(a) leads to an incomplete cancellation

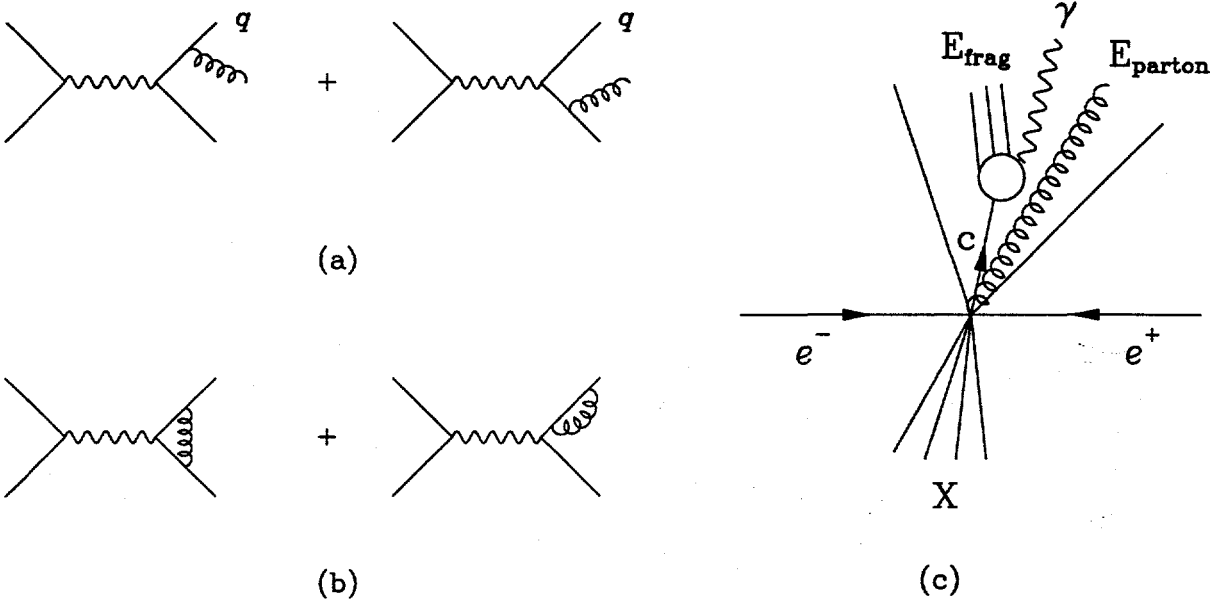


Figure 1: Feynman diagrams are shown in (a) and (b) for the  $\mathcal{O}(\alpha_s)$  cross section  $\hat{\sigma}_{e^+e^- \rightarrow q\bar{q}X}^{(1)}$ ; both real gluon emission diagrams (a) ( $e^+e^- \rightarrow q\bar{q}g$ ) and virtual gluon exchange terms (b) are drawn. In (c), an illustration is presented of an isolation cone containing a parton  $c$  that fragments into a  $\gamma$  plus hadronic energy  $E_{\text{frag}}$ . In addition, the cone includes a gluon that fragments giving hadronic energy  $E_{\text{parton}}$ .

between the two sets. The  $\mathcal{O}(\alpha_s)$  partonic hard part  $\hat{\sigma}_{e^+e^- \rightarrow q\bar{q}X}^{(1)}(x, Q/\mu)$  is therefore not finite when the infrared regulator is removed.

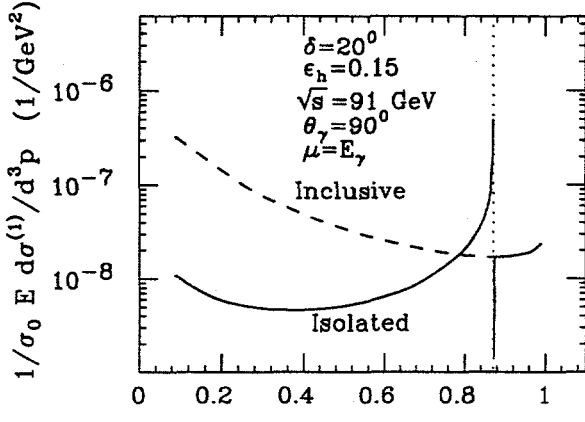
### 3 Breakdown of Conventional Factorization

In this section, we summarize our explicit calculation that demonstrates infrared sensitivity of the partonic hard part for isolated prompt photon production in  $e^+e^- \rightarrow \gamma X$ . It is useful to examine the sketch in Fig. 1(c). In that sketch, we illustrate an isolation cone centered on a  $\gamma$  produced through fragmentation of a parton  $c$ . For the fragmentation contributions, there are two sources of hadronic energy in the isolation cone: i)  $E_{\text{frag}}$  from fragmentation of parton  $c$  itself, and ii)  $E_{\text{partons}}^{\text{cone}}$  from final-state partons other than  $c$  that also happen to be in the cone. The total hadronic energy in the cone is  $E_{\text{hadrons}}^{\text{cone}} = E_{\text{frag}} + E_{\text{partons}}^{\text{cone}}$ . For an isolated  $\gamma$ ,  $E_{\text{hadrons}}^{\text{cone}} \leq E_{\text{cut}}$ , where  $E_{\text{cut}}$  denotes the arbitrary limitation on hadronic energy in the cone that is selected in experiments. We choose to write  $E_{\text{cut}} = \epsilon_h E_\gamma$ , an equation that defines the quantity  $\epsilon_h$ . When the maximum hadronic energy allowed in the isolation cone is saturated by the fragmentation energy,  $E_{\text{cut}} = E_{\text{frag}}$ , there is no allowance for energy in the cone from other final-state partons. In particular, if there is a gluon in the final state, the phase space accessible to this gluon is restricted.

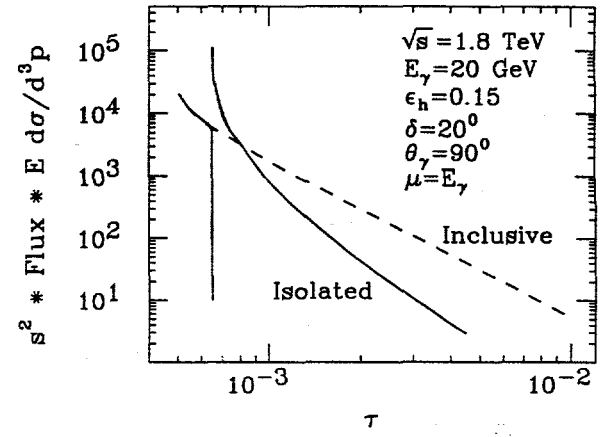
We make frequent use of the variable  $x_\gamma = 2E_\gamma/\sqrt{s}$ , and we define

$$x_{\text{crit}} = \frac{1}{1 + \epsilon_h}. \quad (2)$$

There are three cases of interest:  $x_\gamma < x_{\text{crit}}$ ,  $x_\gamma = x_{\text{crit}}$ , and  $x_\gamma > x_{\text{crit}}$ . Because of the isolation condition, the phase space constraints are different in the three regions. We summarize the physical



(a)



(b)

Figure 2: One-loop quark fragmentation contributions to the isolated and inclusive cross sections (a) as a function of  $x_\gamma = 2E_\gamma/\sqrt{s}$  in  $e^+e^- \rightarrow \gamma X$  at  $\sqrt{s} = 91$  GeV, and (b) as a function of  $\tau$  in  $p\bar{p} \rightarrow \gamma X$  at  $\sqrt{s} = 1.8$  TeV.

situation in the separate regions and show that the next-to-leading order partonic term for quark fragmentation,  $E_q d\hat{\sigma}_{e^+e^- \rightarrow qX}^{iso} / d^3 p_q$ , is infrared sensitive<sup>3</sup> at and below the point  $x_\gamma = 1/(1 + \epsilon_h)$ .

### 3.1 $x_\gamma < 1/(1 + \epsilon_h)$

When  $x_\gamma < 1/(1 + \epsilon_h)$ , subprocesses with two-body final states do not contribute. This statement follows from energy conservation. In a two-body final state,  $E_\gamma + E_{frag} = \sqrt{s}/2$ , and  $E_{hadrons}^{cone} = E_{frag} = (1 - x_\gamma)\sqrt{s}/2$ . Isolation requires  $E_{hadrons}^{cone} \leq \epsilon_h E_\gamma = \epsilon_h x_\gamma \sqrt{s}/2$ . Correspondingly, the two-body final state processes contribute only for  $x_\gamma \geq x_{crit}$ . In particular, since two-body final states are absent, there is no contribution from one-loop virtual gluon exchange diagrams. There is a contribution from the three-body final state real gluon emission diagrams. At the partonic level, these yield a well-known infrared pole singularity having the form  $1/(1 - x_q)$  as  $x_q = x_\gamma/z \rightarrow 1$ . Because the one-loop virtual gluon exchange diagrams do not contribute, the infrared pole singularity remains uncanceled in  $\hat{\sigma}_{e^+e^- \rightarrow qX}^{iso}$ .

If conventional factorization were valid, the fragmentation contributions to the physical cross section would be expressed in the factorized form

$$E_\gamma \frac{d\sigma_{e^+e^- \rightarrow \gamma X}^{iso}}{d^3 \ell} = \sum_c \int_{\max[x_\gamma, \frac{1}{1+\epsilon_h}]}^1 \frac{dz}{z} E_c \frac{d\hat{\sigma}_{e^+e^- \rightarrow cX}^{iso}}{d^3 p_c} \left( x_c = \frac{x_\gamma}{z} \right) \frac{D_{c \rightarrow \gamma}(z, \delta)}{z}; \quad (3)$$

$x_c = 2E_c/\sqrt{s}$ . The sum extends over  $c = q, \bar{q}$  and  $g$ . Function  $D_{c \rightarrow \gamma}(z, \delta)$  is the nonperturbative function that describes fragmentation of parton “ $c$ ” into a photon; its evolution is governed by the Altarelli-Parisi equations. The lower limit of integration results from the isolation requirement with the assumption that all fragmentation energy is in the isolation cone<sup>3</sup>. After convolution with  $D_{q \rightarrow \gamma}(z)$ , the inverse power infrared sensitivity of  $\hat{\sigma}_{e^+e^- \rightarrow qX}^{iso}$ , at the partonic level, yields a logarithmic divergence in the physical cross section  $\sigma_{e^+e^- \rightarrow \gamma X}^{iso}$  proportional to  $\ln(1/x_\gamma - (1 + \epsilon_h))$ . As shown in Fig. 2(a), this means that the isolated cross section would become larger than the inclusive cross section in the vicinity of  $x_\gamma \rightarrow 1/(1 + \epsilon_h)$ , a result that is certainly not physical. This infrared sensitivity in  $\hat{\sigma}_{e^+e^- \rightarrow qX}^{iso}$  signals a clear breakdown of conventional perturbative factorization.

Our claim that conventional perturbative factorization breaks down has been contested<sup>9</sup>. However, a careful reading of that paper shows that, after repeating our derivation, the authors come to the same conclusions as we do. To quote from the concluding paragraph<sup>9</sup>, “the [infrared] logarithms

.. become large in the neighborhood of  $x_\gamma \sim x_{\text{crit}}$  ..."; "one has to study whether these [infrared] logarithms can be factored since they reflect long-distance effects"; and "they destroy the relevance of the perturbative expansion at least in the neighborhood of  $x_{\text{crit}}$ ".

### 3.2 $x_\gamma = 1/(1 + \epsilon_h)$

When  $x_\gamma = 1/(1 + \epsilon_h)$ , it is possible to have  $x_q = x_\gamma/z = 1$ . The one-loop virtual gluon exchange diagrams contribute fully in this case, with contributions proportional to  $\delta(1 - x_q)$ . However, isolation constraints limit the phase space accessible to gluon emission in the real subprocess,  $e^+e^- \rightarrow q\bar{q}g$ . Consequently, the infrared divergences of the real and virtual contributions do not cancel completely in the isolated case, unlike the inclusive case. Working in  $n = 4 - 2\epsilon$  dimensions, after adding the real and virtual contributions, we find<sup>3</sup>

$$E_q \frac{d\hat{\sigma}^{\text{iso}}(\text{real+virtual})}{d^3 p_q} \sim \left\{ \frac{1}{\epsilon^2} + \frac{1}{\epsilon} \left( \frac{3}{2} - \ln \frac{\delta^2}{4} \right) \right\} \delta(1 - x_q) + \text{finite terms}. \quad (4)$$

The presence of the uncanceled  $1/\epsilon$  and  $1/\epsilon^2$  terms means that the regulator  $\epsilon$  cannot be set to 0. Therefore, at  $x_q = 1$ , corresponding to  $x_\gamma = 1/(1 + \epsilon_h)$ , the partonic term for quark fragmentation is infrared divergent, and the perturbative calculation is not well-defined. Conventional perturbative factorization again breaks down.

In Fig. 2(a) we present the perturbatively computed one-loop quark fragmentation contributions to the physical cross sections for inclusive and isolated prompt photon production  $e^+e^- \rightarrow \gamma + X$  at  $\sqrt{s} = 91$  GeV.

### 3.3 Relevance for Experiment

The logarithmic divergence in the physical cross section  $d\sigma^{\text{iso}}/dx_\gamma$  for  $x_\gamma < x_{\text{crit}}$  is an integrable singularity. Data are presented in bins of finite width, related to the experimental resolution. If the perturbative divergence spans a very narrow region in  $x_\gamma$ , one that is smaller than the typical bin width, then the theoretical cross section will still be useful. For the situation examined in this paper, the perturbatively calculated isolated cross section exceeds the inclusive cross section over a region in  $x_\gamma$  that is not narrow. As indicated in Fig. 2(a), the region extends over an interval of about 4 GeV in  $E_\gamma$ , larger than typical bin widths at LEP and SLC. This means that the perturbatively computed  $d\sigma^{\text{iso}}/dx_\gamma$  cannot be accepted at face value. Conventional perturbative QCD leaves strong infrared sensitivity in the partonic hard-part at next-to-leading order, and we must look beyond fixed-order perturbation theory in order to derive an expression that makes physical sense.

### 3.4 Origin and Possible Cure of the infrared Sensitivity

For  $x_\gamma < x_{\text{crit}}$ , the infrared sensitivity of the form  $\frac{1}{1-x_q} \ln(\frac{1}{1-x_q})$  comes from soft real gluon emission. An analogous case is the transverse momentum ( $q_T$ ) distribution for the production of the intermediate vector bosons  $W$  and  $Z$  or of massive lepton-pairs (the Drell-Yan process). At  $\mathcal{O}(\alpha_s)$ , the subprocess  $q + \bar{q} \rightarrow \gamma^* + g$  provides a singular distribution of the form  $\alpha_s/q_T^2$ . Likewise, the thrust distribution in  $e^+e^-$  annihilation,  $d\sigma/dT$ , is singular in the limit  $T \rightarrow 1$ . Fixed-order calculations do not work as  $q_T \rightarrow 0$  or as  $T \rightarrow 1$ , and resummation is invoked<sup>10,11</sup>. For isolated photon production, as discussed in this paper, a similar problem is encountered as  $x_q \rightarrow 1$ , or, equivalently, as  $x_\gamma \rightarrow \frac{1}{1+\epsilon_h}$ . All-orders resummation of soft gluon radiation is therefore also suggested for isolated photon production. Owing to the limited phase space available for gluon radiation, a Sudakov suppression of the infrared divergence might be expected.

While there are similarities, there are also significant differences between the isolated photon case and the  $q_T$  distribution and thrust examples cited above. In the isolated photon case, the point of infrared divergence occurs within the physical region at a location determined by the experimenters' choice of  $\epsilon_h$ , not at a fixed point at the edge of phase space (i.e.,  $q_T = 0$ , and  $T = 1$ ). More

importantly, in the Drell-Yan and thrust examples, the infrared divergence cancels exactly between the real emission and gluon loop diagrams. Absent in these cases are uncanceled  $1/\epsilon^2$  and  $1/\epsilon$  poles that arise in the isolated photon case at  $x_\gamma = x_{\text{crit}}$  from the restricted phase space for real gluon emission, c.f., Eq. (4). In the Drell-Yan and thrust cases, the divergence is regulated, and soft-gluon resummation can be done in Fourier transformed impact parameter space. The uncanceled poles of the isolated photon case would be tantamount to an extra unbalanced  $\delta(q_T^2)$  piece in the Drell-Yan case. For isolated photon production, resummation must be done at the partonic level, in the  $x_q$  distribution, before the convolution is performed with the  $q \rightarrow \gamma X$  fragmentation function. A resummation procedure must be devised to handle the unbalanced  $\delta(1 - x_q)$  problem of Eq. (4).

The presence of infrared sensitivity is a tip-off that non-perturbative effects are present and must be addressed. For example, in the example of the  $q_T$  distribution in Drell-Yan case, non-perturbative functions  $g_i$  are introduced in the implementation of resummation in impact parameter space<sup>10</sup>. These unknown functions determine the behavior of the differential cross section at modest values of  $q_T$ . The critical point  $x_{\text{crit}}$  of the isolated photon case, defined in Eq. (2), is arbitrary since  $\epsilon_h$  is chosen experimentally. If  $\epsilon_h$  is very small,  $x_{\text{crit}} \rightarrow 1$ ; there will be only a very narrow region over which resummation will matter, and fixed-order perturbation theory will be adequate. On the other hand, if we are interested in extracting fragmentation functions from the data,  $\epsilon_h$  must not be too small. There will then be a relatively large region in which non-perturbative functions analogous to  $g_i$  will play a significant role in fits to data. Their presence is a source of uncertainty for the extraction of quark-to-photon fragmentation functions in next-to-leading order. After resummation, instead of the divergence apparent in the solid curve in Fig. 2(a), the predicted isolated cross section below  $x_\gamma = x_{\text{crit}}$  will remain bounded from above by the inclusive prediction, and it will join smoothly at  $x_{\text{crit}}$  to the form it takes in Fig. 2(a) above  $x_{\text{crit}}$ .

### 3.5 Recapitulation for $e^+e^- \rightarrow \gamma + X$

To recapitulate, in  $e^+e^- \rightarrow \gamma + X$ , the next-to-leading order partonic term associated with the quark fragmentation contribution is infrared sensitive when  $x_\gamma \leq 1/(1 + \epsilon_h)$ . Conventional perturbative factorization of the cross section for isolated photon production in  $e^+e^-$  annihilation breaks down in the neighborhood of  $x_\gamma = 1/(1 + \epsilon_h)$ . The isolated cross section, as usually defined, is not an infrared safe observable and cannot be calculated reliably in conventional fixed-order perturbative QCD at, and in the immediate region below,  $x_\gamma = 1/(1 + \epsilon_h)$ . All-orders resummation offers a possible theoretical resolution, but this situation differs in important respects from other examples of successful application of resummation techniques.

## 4 Hadron Collider Experiments

In hadron collisions,  $A + B \rightarrow \gamma X$ , we are interested in the production of isolated prompt photons as a function of the photon's transverse momentum,  $p_T$ . At next-to-leading order in QCD, one must include fragmentation at next-to-leading order. At this order, difficulties analogous to those in  $e^+e^-$  annihilation are encountered also in the hadronic case. To illustrate the problem<sup>3</sup>, we consider the contribution from a quark-antiquark subprocess in which the flavors of the initial and final quarks differ:  $q' + \bar{q}' \rightarrow q + \bar{q} + g$ , where  $q$  fragments to a  $\gamma$ . We keep only final state gluon radiation so that the results of our investigations of  $e^+e^-$  annihilation can be exploited directly. We specialize to rapidity  $y_\gamma = 0$  and take equal values for the incident parton momentum fractions,  $x_a = x_b = x = \sqrt{\tau}$ . In the translation to the hadronic case, the variable  $x_\gamma$  becomes  $\hat{x}_T$  where  $\hat{x}_T = 2p_T/\sqrt{\hat{s}} \sim x_T/x$  with  $x_T = 2p_T/\sqrt{s}$ . The critical point at which infrared divergence is manifest in the  $e^+e^-$  case tends to occur at relatively large values of  $x_\gamma$ . Owing to the correspondence  $x_\gamma \sim x_T/x$ , the critical point in the hadron case occurs at small values of the parton momentum fraction  $x$  where its effects are enhanced by the parton densities.

The special one-loop quark fragmentation contribution to the observed cross section takes the

form

$$E_\gamma \frac{d\sigma_{AB \rightarrow \gamma X}}{d^3 \ell} \sim \int_{x_T^2}^1 d\tau \Phi_{q' \bar{q}'}(\tau) E_\gamma \frac{d\sigma_{q' \bar{q}' \rightarrow \gamma X}}{d^3 \ell}(\tau) + \text{other subprocesses}. \quad (5)$$

In Fig. 2(b), we show the *integrand* in Eq. (5) obtained after convolution with the parton flux  $\Phi(\tau)$ . We compare the integrands for the isolated and the inclusive cases, and we observe again that infrared sensitivity at fixed-order leads to the unphysical result that the isolated integrand exceeds the inclusive integrand. It is evident that the convolution with the parton flux substantially enhances the influence of the region of infrared sensitivity.

The integrand of Eq. (5) is not a physical observable. Instead, the contribution to the hadronic cross section is the area under the curve in Fig. 2(b) from  $x_T^2$  to 1. The divergences above and below the point  $\hat{x}_T = 1/(1 + \epsilon_h)$  [or  $\sqrt{\tau} = x_T(1 + \epsilon_h)$ ] are integrable logarithmic divergences, and thus they yield a finite contribution if an integral is done over all  $\tau$ . Indeed, after integration, the calculated isolated cross section may well turn out less than its inclusive counterpart since the unwarranted extra positive contribution associated with the logarithmic divergence in the region of small  $\tau$  may be more than compensated by the area between the inclusive and the isolated curves at large  $\tau$ . The issue is one of reliability. We stress that the perturbatively calculated one-loop partonic cross section  $E_q d\hat{\sigma}_{q' \bar{q}' \rightarrow q X}^{iso}/d^3 p_q$ , has an inverse-power divergence as  $x_q \rightarrow 1$  and has uncanceled  $1/\epsilon^2$  and  $1/\epsilon$  poles in dimensional regularization<sup>3</sup>. This pole divergence for  $\hat{x}_T < 1/(1 + \epsilon_h)$  becomes a logarithmic divergence in  $E_\gamma d\sigma_{q' \bar{q}' \rightarrow \gamma X}/d^3 \ell$  after the convolution with a long-distance  $q \rightarrow \gamma X$  fragmentation function. Although the logarithmic divergence near  $\sqrt{\tau} = x_T(1 + \epsilon_h)$  is integrable, the isolated integrand should never exceed the inclusive integrand. It is not correct to accept at face value a prediction for an isolated cross section obtained from a perturbatively calculated integrand whose value exceeds that appropriate for the inclusive case (even if, after integration over  $\tau$ , the resulting isolated cross section is smaller than the inclusive).

In the calculated isolated cross section, how large is the uncertainty associated with the infrared sensitivity of the next-to-leading order quark fragmentation terms? Referring to Fig. 2(b), we define the overestimate of the isolated cross section to be the area under the solid curve but above the dashed curve. We define the maximum isolated cross section to be the area under the lower of the solid and dashed curves. Doing so, we find that the next-to-leading order quark-fragmentation contribution to the physical isolated cross section is overestimated by 54%. While this overestimate is certainly large, one should bear in mind that the tree-level fragmentation contribution is not affected by the infrared uncertainty and that the tree-level term is larger than the one-loop quark fragmentation term that is of concern. Thus, the uncertainty in the overall fragmentation contribution will be typically only some fraction of 54%. Second, even though fragmentation may account for half or more of the inclusive prompt photon yield at relatively small values of  $p_T$ , the fragmentation fraction is substantially reduced by isolation. We suggest therefore, that the net uncertainty in the physical isolated cross section associated with the next-to-leading order fragmentation terms may be at the 10% level.

## 5 Summary

The results in both the  $e^+e^-$  and hadronic cases challenge us to find a modified factorization scheme and/or to devise more appropriate infrared safe observables.

## Acknowledgments

Work at Argonne National Laboratory is supported in part by the U. S. Department of Energy, Division of High Energy Physics, Contract No. W-31-109-ENG-38.

## References

1. J. C. Collins, D. E. Soper, and G. Sterman, in *Perturbative Quantum Chromodynamics*, ed. A. H. Mueller (World Scientific, Singapore, 1989).
2. E. L. Berger, X. F. Guo, and J. W. Qiu, *Phys. Rev. D* **53**, 1124 (1996).
3. E. L. Berger, X. F. Guo, and J. W. Qiu, *Phys. Rev. Lett.* **76**, 2234 (1996); *Phys. Rev. D* **54**, 5470 (1996).
4. P. Aurenche *et al*, *Nucl. Phys. B* **399**, 34 (1993) and references therein; H. Baer, J. Ohnemus, and J. F. Owens, *Phys. Rev. D* **42**, 61 (1990); E. L. Berger and J. W. Qiu, *Phys. Lett. B* **248**, 371 (1990) and *Phys. Rev. D* **44**, 2002 (1991); L. Gordon and W. Vogelsang, *Phys. Rev. D* **50**, 1901 (1994); L. Gordon, Argonne report ANL-HEP-PR-96-60 (hep-ph/9611391), November, 1996.
5. ALEPH Collaboration, D. Buskulic *et al*, *Z. Phys. C* **57**, 17 (1993) and references therein; DELPHI Collaboration, P. Abreu *et al*, *Z. Phys. C* **69**, 1 (1995) and references therein; L3 Collaboration, M. Acciarri *et al*, *Phys. Lett. B* **388**, 409 (1996) and references therein; OPAL Collaboration, G. Alexander *et al*, *Z. Phys. C* **71**, 1 (1996) and references therein.
6. K. Koller, T. F. Walsh, and P. M. Zerwas, *Z. Phys. C* **2**, 197 (1979); E. Laermann, T. F. Walsh, I. Schmitt, and P. M. Zerwas, *Nucl. Phys. B* **207**, 205 (1982); E. W. N. Glover and A. G. Morgan, *Z. Phys. C* **62**, 311 (1994); G. Kramer and B. Lampe, *Z. Phys. C* **34**, 497 (1987) and *Phys. Lett. B* **269**, 401 (1991); G. Kramer and H. Spiesberger, *Proceedings of Annecy Workshop on Photon Radiation from Quarks*, Annecy, France, December 1991, CERN report CERN 92-04, ed. S. Cartwright, pp. 26-40; P. Mättig, H. Spiesberger, and W. Zeuner, *Z. Phys. C* **60**, 613 (1993).
7. E. L. Berger, X. F. Guo, and J. W. Qiu, in *The Fermilab Meeting*, Proceedings of the 7th Meeting of the Division of Particles and Fields of the American Physical Society, Fermilab, November, 1992; ed. C. H. Albright, P. H. Kasper, R. Raja, and J. Yoh (World Scientific, Singapore, 1993), pp. 957-960.
8. ALEPH Collaboration, D. Buskulic *et al*, *Z. Phys. C* **69**, 365 (1996); OPAL Collaboration, K. Ackerstaff *et al*, CERN report CERN-PPE/97-086 (July, 1997), submitted to *Z. Phys. C*.
9. P. Aurenche, M. Fontannaz, J. Ph. Guillet, A. Kotikov, and E. Pilon, *Phys. Rev. D* **55**, 1124 (1997).
10. J. C. Collins, D. E. Soper, and G. Sterman, *Nucl. Phys. B* **250**, 199 (1985). For a recent treatment and list of references, see R. K. Ellis, D. A. Ross, and S. Veseli, Fermilab report FERMILAB-PUB-97/082-T (hep-ph/9704239), April, 1997.
11. M. Greco and Y. Srivastava, *Phys. Rev. D* **23**, 2791 (1981); S. Catani, G. Turnock, B. R. Webber, and L. Trentadue, *Phys. Lett. B* **263**, 491 (1991); G. Sterman, in *QCD and Beyond*, Theoretical Advanced Study Institute in Elementary Particle Physics (TASI'95), June, 1995, ed. D. E. Soper (World Scientific, Singapore, 1995).